Spectral characterization of magic angles in twisted bilayer graphene

Simon Becker,[1,*] Mark Embree,[2,†] Jens Wittsten [3,‡] and Maciej Zworski [4,§]

[1]*Department of Applied Mathematics and Theoretical Physics, University of Cambridge, Wilberforce Road, Cambridge CB3 0WA, United Kingdom*
[2]*Department of Mathematics, Virginia Tech, Blacksburg, Virginia 24061, USA*
[3]*Centre for Mathematical Sciences, Lund University, Box 118, SE-221 00 Lund, Sweden and Department of Engineering, University of Borås, SE-501 90 Borås, Sweden*
[4]*Department of Mathematics, University of California, Berkeley, California 94720, USA*

Twisted bilayer graphene (TBG) has been experimentally observed to exhibit almost flat bands when the twisting occurs at certain *magic angles*. In this Letter we show that in the approximation of vanishing AA coupling, the magic angles (at which there exist entirely flat bands) are given as the eigenvalues of a non-Hermitian operator, and that all bands start squeezing exponentially fast as the angle θ tends to 0. In particular, as the interaction potential changes, the dynamics of magic angles involves the nonphysical complex eigenvalues. Using our new spectral characterization, we show that the equidistant scaling of inverse magic angles is special for the choice of tunneling potentials in the continuum model, and is not protected by symmetries. While we also show that the protection of zero-energy states holds in the continuum model as long as particle-hole symmetry is preserved, we observe that the existence of flat bands and the exponential squeezing are special properties of the chiral model.

I. INTRODUCTION

The electronic structure in a stack of two graphene sheets depends crucially on the relative twist angle θ of the layers [1–8]. Tunneling interactions coming from long-period moiré patterns (emerging from the twisting) cause the Dirac dispersion relation of the noninteracting sheets to change dramatically: the Floquet bands become nearly flat at a certain discrete set of *magic angles*, as observed in Refs. [9–11]. This flattening of bands led to the discovery of Mott insulation [12] and of unconventional superconductivity in TBG [13–16]. The number and distribution of higher-order magic angles is still not fully understood [17,18].

We give a new spectral characterization of magic angles for the reduced model without AA coupling (*chiral model* of Ref. [19]) as eigenvalues of a compact non-Hermitian Birman-Schwinger operator. Since its spectrum has also complex eigenvalues, we establish that flat bands also exist for complex parameters in the continuum model. The spectral characterization also allows an efficient numerical calculation of a large set of magic angles, as demonstrated in Ref. [20, §5]. Consequently, we are able to study a larger number of magic angles and find that the equidistant spacing of reciprocal angles observed in Ref. [19] is unique to the particular tunneling potential and not protected by symmetries—see Figs. 1 and 2. In addition, we show that in the chiral model the lowest bands become exponentially small as the inverse twisting angle θ^{-1}

tends to infinity; see also Ref. [21] for an experimental study of small twist angles.

We then analyze the particle-hole symmetric continuum model with additional AA coupling. Based on a numerical analysis of this model and a rigorous argument for the extremal model with only AA coupling (*antichiral model* of Ref. [19]), we find that, unlike in the chiral model, there are no entirely flat bands at zero energy, and bands are also no longer squeezed with an exponential rate. However, we show that the zero energy level of the model with particle-hole symmetry, is still protected in the spectrum, which has been previously observed in Ref. [19] for the chiral model.

II. CONTINUUM MODEL

The Hamiltonian of the continuum model for twisted bilayer graphene is defined for variables

$$z = x_1 + ix_2, \quad D_{\bar{z}} = \tfrac{1}{2i}(\partial_{x_1} + i\partial_{x_2}), \quad \omega = e^{2\pi i/3},$$

coupling parameters $w = (w_0, w_1)$ and twisting angles φ of the moiré Dirac cones, which we allow to vary independently from the mechanical twisting angle θ, which depends on tunneling parameters w_0, w_1, by

$$H(w, \varphi) := \begin{pmatrix} C(w_0) & D(w_1, \varphi)^* \\ D(w_1, \varphi) & C(w_0) \end{pmatrix}, \tag{1}$$

where

$$D(w_1, \varphi) := \begin{pmatrix} 2e^{i\varphi/2}D_{\bar{z}} & w_1 U(z) \\ w_1 U(-z) & 2e^{-i\varphi/2}D_{\bar{z}} \end{pmatrix},$$

$$C(w_0) := \begin{pmatrix} 0 & w_0 V(z) \\ w_0 V(-z) & 0 \end{pmatrix}. \tag{2}$$

*simon.becker@damtp.cam.ac.uk
†embree@vt.edu
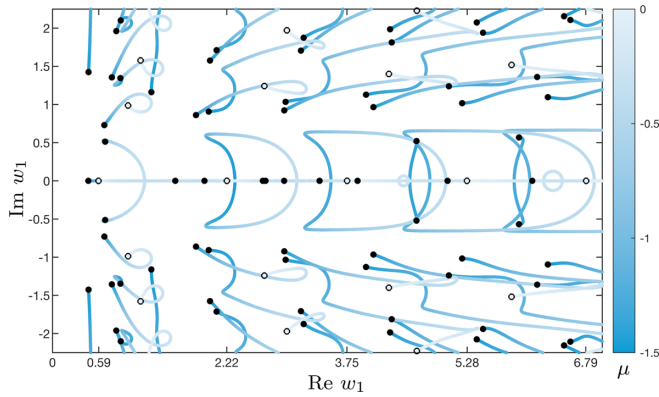‡jens.wittsten@math.lu.se
§zworski@math.berkeley.edu

FIG. 1. For a tunneling potential U_μ in (9) we find nonequidistant spacing of the inverse magic angles: ● denote w_1 for $\mu = -1.5$; the paths trace the w_1 dynamics for $-1.5 \leqslant \mu \leqslant 0$; ○ denote the w_1 for $\mu = 0$.

FIG. 2. Reciprocals of magic angles for potential (3) from Ref. [19] in the complex plane: resonant w_1 (○) come from the full spectrum of the operator (6) defining magic angles, and the (real-valued) magic w_1 (+) are the reciprocals of the *physically relevant* positive angles.

Here, the tunneling potentials [9,19] are given by

$$U(z) := \sum_{k=0}^{2} \omega^k e^{\frac{1}{2}(z\bar\omega^k - \bar z \omega^k)}, \text{ and } V(z) := 2\partial_z U(z). \quad (3)$$

The parameter w_0 controls the AA-coupling and w_1 controls AB and BA coupling. The Hamiltonian with only AB and BA coupling, w_0, is called the *chiral* continuum model and w_0^{-1} is proportional to θ. The opposite choice of only AA coupling, w_1, is called the *antichiral* continuum model and w_1^{-1} is proportional to θ. For both the chiral and antichiral model, a simple conjugation removes the dependence on φ and we may just assume $\varphi = 0$. The choice $\varphi = 0$ is the *particle-hole symmetric* continuum model. The potential U satisfies three key symmetry properties:

$$U\left(z + \tfrac{4}{3}\pi i \omega^\ell\right) = \bar\omega U(z) \text{ for } \ell = 1, 2, \quad (4a)$$

$$U(\omega z) = \omega U(z), \quad \overline{U(\bar z)} = U(z), \quad (4b)$$

and most of the results here apply to more general potentials satisfying (4), for instance, (9). Such potentials are discussed in the Supplemental Material, see Ref. [22, (24)].

It is immediate from (4) that the Hamiltonian is periodic with respect to the lattice $\Gamma := 4\pi(i\omega\mathbb{Z} \oplus i\omega^2\mathbb{Z})$, and by Floquet theory magic angles are defined as angles $\theta = w_1^{-1}$ such that the energy 0 is in the spectrum (on Γ-periodic functions) of all Hamiltonians $H_\mathbf{k}(w, \varphi)$, where

$$H_\mathbf{k}(w, \varphi) := \begin{pmatrix} C(w_0) & D(w_1, \varphi)^* - \bar{\mathbf{k}} \\ D(w_1, \varphi) - \mathbf{k} & C(w_0) \end{pmatrix}, \quad (5)$$

where $\mathbf{k} \in \mathbb{C}$ denotes the quasimomentum.

The Mott insulation, experimentally observed in TBG [12], is due to strongly correlated electron interactions [23]; the exponential squeezing of bands described here provides a qualitative explanation for said effect, as kinetic energy in squeezed bands and electronic interactions dominate [24]. In addition, it has been observed [14,15] that the correlated insulating and superconducting regimes are not limited to magic angles but persist also at angles close to the magic ones, as long as bands remain narrow. This suggests that the physically relevant phenomenon is the squeezing and flattening of
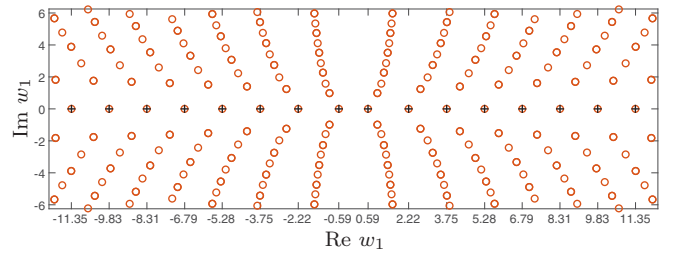
bands, rather than the existence of an entirely flat band (which is seemingly unstable under perturbations). To understand this better, we recall the Bardeen-Cooper-Schrieffer (BCS) theory which postulates that the critical temperature for the phase transition into the superconducting regime satisfies $T_c \propto \exp(-\frac{1}{U n_0(E_F)})$ where $n_0(E_F)$ is the density of states at the Fermi energy. The exponential squeezing of bands therefore leads to a macroscopically increased density of states which raises the critical temperature.

Spectral characterization of magic angles. To obtain a spectral characterization of magic angles for the chiral Hamiltonian, we define the *Birman-Schwinger operator* for $\mathbf{k} \notin \Gamma^*$ (the dual lattice) by

$$T_\mathbf{k} := (2D_{\bar z} - \mathbf{k})^{-1} \begin{pmatrix} 0 & U(z) \\ U(-z) & 0 \end{pmatrix}. \quad (6)$$

For zero AA coupling, there is a discrete set of values $w_1 \in \mathcal{A} := 1/\text{Spec}(T_\mathbf{k})$, where Spec denotes the spectrum (always on Γ-periodic functions), that is, quite remarkably, independent of $\mathbf{k} \notin \Gamma^*$ [20, Theorem 2]. In addition, the set $\mathcal{A}$ satisfies symmetries $\mathcal{A} = -\mathcal{A} = \overline{\mathcal{A}}$ [20, Proposition 3.2]; see Figs. 1 and 2.

The flat bands at zero of the chiral Hamiltonian then occur precisely at $w_1 \in \mathcal{A}$. The set of magic angles is then just given by angles θ for which $\theta^{-1} \in \mathcal{A} \cap \mathbb{R}$, see Ref. [20, Theorem 2] for details.

The spectral characterization allows efficient calculation of the set $\mathcal{A}$, see below. The following trace for the potential (3)

$$\text{tr}\, T_\mathbf{k}^4 = \sum_{\alpha \in \mathcal{A}} \alpha^{-4} = \frac{72\pi}{\sqrt{3}} \quad (7)$$

can be calculated explicitly [20, §3.3] and that shows that the set $\mathcal{A}$ is nontrivial in that case.

In addition, we can characterize the magic angles for the chiral model by analyzing the spectrum of the non-Hermitian operator $D(w_1) = D(w_1, 0)$ in (2). In fact, $\theta = w_1^{-1}$ is a magic angle if and only if $\text{Spec}(D(w_1)) = \mathbb{C}$. For all other θ, $\text{Spec}(D(w_1)) = \Gamma^*$, the dual lattice [20, Theorem 2]. Figure 3 illustrates this remarkable discontinuity in the spectrum of $D(w_1)$.

Asymptotic distribution of magic angles. It has been observed in Ref. [19] that the differences of reciprocal magic angles, with $0 < \theta_k < \theta_{k-1}$, for the chiral model behave asymptotically like $\theta_k^{-1} - \theta_{k-1}^{-1} \simeq 3/2$. Our new characterization
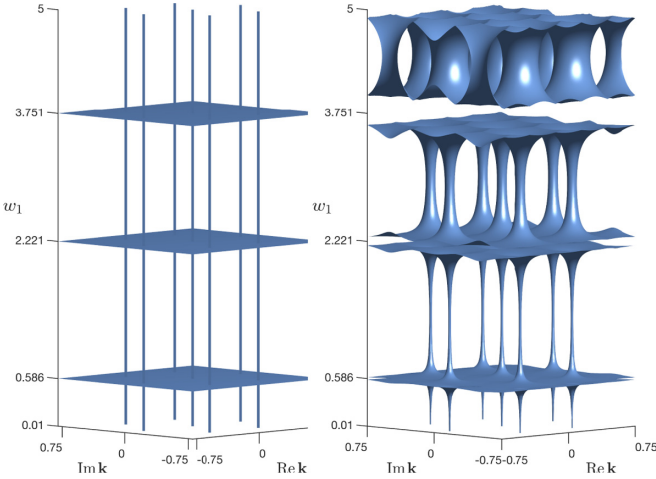
FIG. 3. (left panel) The spectrum of $D(w_1)$ (in the $\mathbf{k}$ plane) as w_1 varies (vertical axis). Flat surfaces indicate that $1/w_1$ is a magic angle. (right panel) Level surface of $\|(D(w_1) - \mathbf{k})^{-1}\| = 10^{\frac{9}{4}}$ as a function of $\mathbf{k}$ and w_1: the norm blows up at magic angles for all $\mathbf{k}$ (w_1 near 0.586, 2.221, and 3.751). The thickening of the "trunks" reflects the exponential squeezing of the smallest eigenvalue of $H_{\mathbf{k}}((0, w_1), 0)$ as w_1 grows, relating to *pseudospectral* effects [25,26]—see (10) and the discussion that follows.

of magic angles as real eigenvalues of the operator $T_{\mathbf{k}}$ can give magic angles to high precision: we have high confidence of all the digits shown in Table I. This gives a refined asymptotic behavior (see Ref. [20, §5])

$$\theta_k^{-1} - \theta_{k-1}^{-1} \simeq 1.515, \quad k \leqslant 13. \tag{8}$$

This calls to question a recently suggested WKB approach [27]: the explanation proposed there gives the asymptotic spacing of magic angles as $\theta_k^{-1} - \theta_{k-1}^{-1} \simeq 1.47$. In addition, the approach proposed in Ref. [27] would seemingly apply to all tunneling potentials satisfying (4) in the chiral model. However, the equidistant asymptotic distribution of magic angles is not stable under such perturbations, as we discuss in our next paragraph.

TABLE I. Reciprocals of the magic angles θ_k, and the gaps between those reciprocals.

k	θ_k^{-1}	$\theta_k^{-1} - \theta_{k-1}^{-1}$
1	0.58566355838955	
2	2.2211821738201	1.6355
3	3.7514055099052	1.5302
4	5.276497782985	1.5251
5	6.79478505720	1.5183
6	8.3129991933	1.5182
7	9.829066969	1.5161
8	11.34534068	1.5163
9	12.8606086	1.5153
10	14.376072	1.5155
11	15.89096	1.5149
12	17.4060	1.5150
13	18.920	1.5147

Lattice relaxations. It has been proposed in Ref. [28] that to take lattice relaxation effects into account more general tunneling potentials should be considered in the continuum model. We therefore consider the simplest generalization of the tunneling potential U (3) which still satisfies (4):

$$U_\mu(z) := U(z) + \mu \sum_{k=0}^{2} \omega^k e^{\bar{z}\omega^k - z\bar{\omega}^k}, \quad \mu \in \mathbb{R}. \tag{9}$$

In this case, flat bands are still given as the eigenvalues of the respective Birman-Schwinger operator (6), with U replaced by U_μ. However, the equidistant spacing of magic angles is no longer visible. See Fig. 1, which also indicates that, to understand the dynamics of θ as μ varies, complex values must be considered. If we abandon the *reality* requirement that $\overline{U(\bar{z})} = U(z)$ in (4), a generic U will not have any *real* magic angles.

Point-localized states and exponential squeezing of bands From (8) we see that magic angles in the chiral model accumulate close to the zero twisting angle. However, aside from an accumulation of magic angles as $\theta \downarrow 0$, we also discover an exponential squeezing of eigenvalues of the chiral Floquet Hamiltonian $H_{\mathbf{k}}((0, w_1), \varphi)$, $\varphi \leqslant C/w_1$, to zero. In the chiral model, the low-lying bands for small angles become asymptotically flat: if $\{E_j(\mathbf{k}, w_1)\}_{j=0}^{\infty} =$ Spec$(H_{\mathbf{k}}((0, w_1), \varphi)) \cap [0, \infty)$, $E_{j+1} \geqslant E_j$, then there are constants $c_0, c_1, c_2 > 0$ such that

$$|E_j(\mathbf{k}, w_1)| \leqslant c_0 e^{-c_1 w_1}, \quad j \leqslant c_2 w_1, \tag{10}$$

see Fig. 4. In fact, numerical results here suggest that $c_1 = 1$ and c_2 can be taken arbitrarily large.

To understand the squeezing of low-lying eigenvalues theoretically, we use a semiclassical reformulation of the Hamiltonian of the chiral model. To study the nullspace of $H_{\mathbf{k}}((0, w_1), 0)$, it suffices to study effective two-by-two operators $D(w_1, 0)$ in (2). The principal Weyl symbol of $D(w_1, 0)$, cf. [29, p. 213], is given in terms of phase-space variables $z = x_1 + ix_2$ and $2\zeta = \xi_1 - i\xi_2$ by

$$\sigma(D(w_1, 0))(z, \bar{z}, \bar{\zeta}) = \begin{pmatrix} 2\bar{\zeta} & w_1 U(z) \\ w_1 U(-z) & 2\bar{\zeta} \end{pmatrix}. \tag{11}$$

Let q be the determinant of this symbol. Then at points (z^0, ζ^0) in phase space at which $q(z^0, \zeta^0) = 0$ and $\zeta^0 \neq 0$, we then find that the Poisson bracket $\{q, \bar{q}\}(z^0, \zeta^0) \neq 0$ is nonvanishing.

An adaptation of Hörmander's bracket condition to the analytic case [25, Theorem 1.2] implies that, for z^0 away from the set shown in Fig. 5, there exist smooth functions v_h such that $|D(w_1, h)v_h(z)| \leqslant e^{-\frac{c}{h}}$ ($h \leqslant C/w_1$), which are localized to z^0, i.e., $v_h(z^0) = 1$ and $|v_h(z)| \leqslant e^{-\frac{c}{h}|z-z^0|^2}$, see Ref. [20, Theorem 3].

However, the above argument does not apply to the Hamiltonian of the full continuum model (1) while in the antichiral model ($w_1 = 0$) there are no localized modes at z^0 with $U(z^0)U(-z^0) \neq 0$—see Theorem 2 in the Supplemental Material [22]. This is confirmed by numerics: Fig. 6 shows that there is no exponential squeezing of bands.

Symmetries and protected states at zero. Magic angles in the chiral continuum model are the reciprocals of coupling constants w_1 for which 0 is in the spectrum of all $H_{\mathbf{k}}((0, w_1), 0)$.
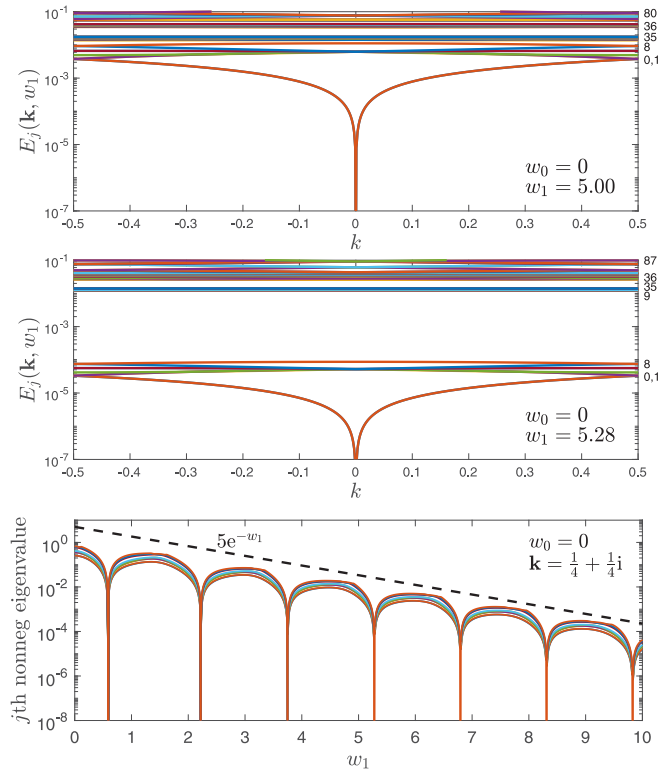
FIG. 4. (top) The smallest non-negative eigenvalues of $H_{\mathbf{k}}((0, w_1), 0)$, $w_1 = 5$, $\mathbf{k} = k\omega/\sqrt{3}$, $-\frac{1}{2} \leqslant k \leqslant \frac{1}{2}$. Selected j values are given in the right margin. (middle) The same, but with $w_1 = 5.28$ nearer the fourth magic w_1 value, showing the marked decrease of the nine lowest bands. (bottom) $E_j(\mathbf{k}, w_1)$ (log scale) for $\mathbf{k} = \frac{1}{4} + \frac{1}{4}i$ and $0 \leqslant j \leqslant 8$. We see (10) with $c_1 = 1$.

We show that the symmetries of the continuum model with particle-hole symmetry imply that the zero energy level is protected in the spectrum of the Hamiltonian for all $w = (w_0, w_1)$.

We start by stating the most straightforward symmetries: translational symmetry

$$\mathscr{L}_{\mathbf{a}} := \mathscr{U}L_{\mathbf{a}}, \quad \mathscr{U} := \operatorname{diag}(\omega, 1, \omega, 1), \quad \mathbf{a} = \frac{4}{3}\pi i\omega^\ell, \quad (12)$$

and rotational C_3 symmetry

$$\mathscr{C}\mathbf{u}(z) = \operatorname{diag}(I_{\mathbb{C}^2}, \bar{\omega}I_{\mathbb{C}^2})\mathbf{u}(\omega z).$$
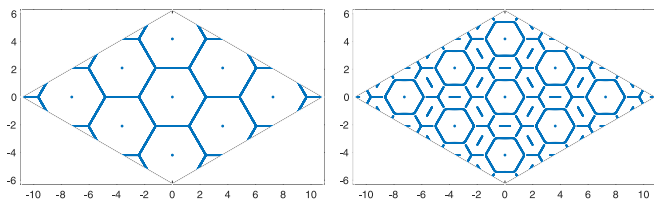

FIG. 5. Plots showing where the bracket $i\{q, \bar{q}\}$ is zero, where q is the determinant of the symbol (11) with U given by (3) (left) and by (9) with $\mu = -2$ (right). The bracket is nonzero, except on a one-dimensional graph and on a set of points.
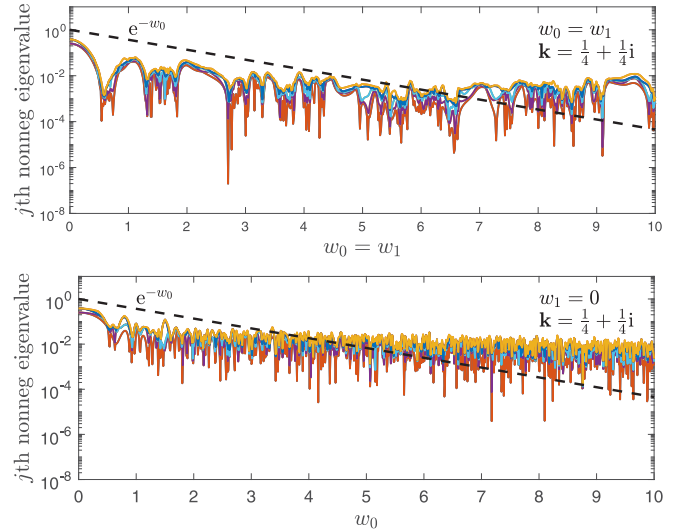

FIG. 6. (top) For $w_0 = w_1 \gg 1$, $\varphi = 0$, no exponential rate of squeezing ($1 \leqslant j \leqslant 10$). The bands show a squeezing effect near $w_0 = w_1 \simeq 0.586$. (bottom) No squeezing for $w_1 = 0$ and $w_0 \gg 1$, consistent with the absence of localized modes and perfectly flat bands.

From $\mathscr{C}\mathscr{L}_{\mathbf{a}} = \mathscr{L}_{\bar{\omega}\mathbf{a}}\mathscr{C}$, we can construct an action, for $\Gamma_3 = (\Gamma/3)/\Gamma$, of the Heisenberg group over $\mathbb{Z}_3$:

$$G := \Gamma_3 \rtimes \mathbb{Z}_3, \quad (\mathbf{a}, k) \cdot (\mathbf{a}', \ell) = (\mathbf{a} + \bar{\omega}\mathbf{a}', k+\ell), \quad (\mathbf{a}, \ell) \cdot \mathbf{u}$$
$$:= \mathscr{L}_{\mathbf{a}}\mathscr{C}^\ell \mathbf{u}. \quad (13)$$

Since there are eleven irreducible representations, see Ref. [20, §2.2], we can decompose the space of square-integrable functions $L^2(\mathbb{C}/\Gamma; \mathbb{C}^4)$ into eleven orthogonal subspaces. For $(k, p) \in \mathbb{Z}_3^2$ we have that nine of these spaces, $L_{k,p}^2$, are characterized by the action $\mathscr{L}_{\mathbf{a}}|_{L_{k,p}^2} = \omega^{k(a_1+a_2)}$ and $\mathscr{C}|_{L_{k,p}^2} = \bar{\omega}^p$. It is then a simple observation that for $w = (w_0, w_1) = 0$ we have that $H(w, 0)e_i = 0$ for $i = 1, \ldots, 4$ and $e_1 \in L_{1,0}^2, e_2 \in L_{0,0}^2, e_3 \in L_{1,1}^2, e_4 \in L_{0,1}^2$ are all in different subspaces. To see that these elements are protected we require mirror, $\mathcal{PT}$, and particle-hole symmetry, see Refs. [30,31] which we discuss in detail in the Supplemental Material: Mirror symmetry $\mathscr{M} : L_{k,p}^2 \to L_{-k+1,-p+1}^2$ [22, Lemma 2],

$$\mathscr{M}\mathbf{u}(z) := \begin{pmatrix} 0 & \sigma_1 \\ \sigma_1 & 0 \end{pmatrix}\mathbf{u}(\bar{z}),$$

and $\mathcal{PT}$ symmetry $\mathcal{PT} : L_{k,p}^2 \to L_{k,-p+1}^2$ [22, Lemma 3],

$$\mathcal{PT}\mathbf{u}(z) = \begin{pmatrix} 0 & I_{\mathbb{C}^2} \\ I_{\mathbb{C}^2} & 0 \end{pmatrix}\overline{\mathbf{u}(-z)}.$$

All of the above symmetries commute with $H(w, \varphi)$, also for $\varphi \neq 0$. Only when setting $\varphi = 0$, the Hamiltonian exhibits, in addition, particle-hole symmetry $\mathscr{S} : L_{k,p}^2 \to L_{-k+1,p}^2$, such that $\mathscr{S}H(w, 0) = -H(w, 0)\mathscr{S}$, where

$$\mathscr{S}\mathbf{u}(z) = \begin{pmatrix} \sigma_2 & 0 \\ 0 & \sigma_2 \end{pmatrix}\mathbf{u}(-z).$$

From the application of the last three symmetries, we find $L_{k,p}^2 \xrightarrow{\mathscr{S}} L_{-k+1,p}^2 \xrightarrow{\mathscr{M}} L_{k,-p+1}^2 \xrightarrow{\mathcal{PT}} L_{k,p}^2$, see Lemma 4 of

Ref. [22], which shows that $\mathrm{Spec}_{L^2_{\bar{k},p}}(H) = -\mathrm{Spec}_{L^2_{\bar{k},p}}(H)$. Recalling the kernel for $w = (0,0)$, we conclude that $\ker_{L^2_{\bar{k},p}} H(w,0) \neq \{0\}$, $k, p \in \{0,1\}$, $w \in \mathbb{R}^2$.

Absence of flat bands. Unlike for the chiral model, which exhibits infinitely many flat bands, perfectly flat bands at zero are absent once AA coupling is switched on. To understand this in the extremal antichiral case, we follow an idea of Thomas [32–35] for Schrödinger operators. First, observe that $0 \in \mathrm{Spec}(H_{\mathbf{k}})$ is equivalent to $\ker Q_{\mathbf{k}} \oplus \ker Q_{\mathbf{k}}^* \neq \{0\}$ (see Ref. [22, Theorem 1] for details), where

$$Q_{\mathbf{k}}(w_0) := \begin{pmatrix} w_0 e^{i\varphi/2} V(z,\bar{z}) & (2D_z + \bar{\mathbf{k}}) \\ (2D_{\bar{z}} + \mathbf{k}) & w_0 e^{i\varphi/2} \overline{V(z,\bar{z})} \end{pmatrix}.$$

By squaring the operators, we find the identity

$$Q_{\mathbf{k}}(Q_{\mathbf{k}} + V_{11}) = [D_x + (k_1,k_2)]^2 I_{\mathbb{C}^2} + V_{12},$$
$$Q_{\mathbf{k}}^*(Q_{\mathbf{k}}^* + V_{21}) = [D_x + (k_1,k_2)]^2 I_{\mathbb{C}^2} + V_{22}, \quad (14)$$

for the momentum operator $D_x = \frac{1}{i}(\partial_{x_1}, \partial_{x_2})$ and auxiliary potentials $V_{ij} = V_{ij}(\beta)$. If we then *complexify* the quasi-

momentum k_1, self-adjointness of the momentum operator implies $\{[D_x + (k_1,k_2)]^2\}^{-1} = \mathcal{O}_{L^2 \to L^2}(|\mathrm{Im}\,k_1|^{-2})$ such that, by (14), $\ker Q_{\mathbf{k}} \oplus \ker Q_{\mathbf{k}}^* = \{0\}$ for $|\mathrm{Im}\,k_1| \gg 1$. Thus, if there was a flat band such that $0 \in \mathrm{Spec}(H_{\mathbf{k}})$, $(k_1,k_2) \in \mathbb{R}^2$ this would imply that $0 \in \mathrm{Spec}(H_{\mathbf{k}})$, $\mathbf{k} = (k_1,k_2) \in \mathbb{C} \times \mathbb{R}$ and thus $\ker Q_{\mathbf{k}} \oplus \ker Q_{\mathbf{k}}^* \neq \{0\}$ $(k_1,k_2) \in \mathbb{C} \times \mathbb{R}$, which is impossible. Details are provided in Ref. [22, Theorem 1].

[1] E. J. Mele, Phys. Rev. B **81**, 161405(R) (2010).

[2] G. Trambly de Laissardiére, D. Mayou, and L. Magaud, Nano Lett. **10**, 804 (2010).

[3] S. Shallcross, S. Sharma, E. Kandelaki, and O. A. Pankratov, Phys. Rev. B **81**, 165105 (2010).

[4] E. Suarez Morell, J. D. Correa, P. Vargas, M. Pacheco, and Z. Barticevic, Phys. Rev. B **82**, 121407(R) (2010).

[5] P. Moon and M. Koshino, Phys. Rev. B **85**, 195458 (2012).

[6] G. Trambly de Laissardiére, D. Mayou, and L. Magaud, Phys. Rev. B **86**, 125413 (2012).

[7] P. Moon and M. Koshino, Phys. Rev. B **87**, 205404 (2013).

[8] D. Weckbecker, S. Shallcross, M. Fleischmann, N. Ray, S. Sharma, and O. Pankratov, Phys. Rev. B **93**, 035452 (2016).

[9] R. Bistritzer and A. H. MacDonald, Proc. Natl. Acad. Sci. USA **108**, 12233 (2011).

[10] R. Bistritzer and A. H. MacDonald, Phys. Rev. B **84**, 035440 (2011).

[11] J. M. B. Lopes dos Santos, N. M. R. Peres, and A. H. Castro Neto, Phys. Rev. B **86**, 155449 (2012).

[12] Y. Cao, V. Fatemi, A. Demir, S. Fang, S. L. Tomarken, J. Y. Luo, J. D. Sanchez-Yamagishi, K. Watanabe, T. Taniguchi, E. Kaxiras, R. C. Ashoori, and P. Jarillo-Herrero, Nature (London) **556**, 80 (2018).

[13] Y. Cao, V. Fatemi, S. Fang, K. Watanabe, T. Taniguchi, E. Kaxiras, and P. Jarillo-Herrero, Nature (London) **556**, 43 (2018).

[14] M. Yankowitz, S. Chen, H. Polshyn, Y. Zhang, K. Watanabe, T. Taniguchi, D. Graf, A. F. Young, and C. R. Dean, Science **363**, 1059 (2019).

[15] Y. Saito *et al.*, Nat. Phys. **16**, 926 (2020).

[16] H. C. Po, L. Zou, A. Vishwanath, and T. Senthil, Phys. Rev. X **8**, 031089 (2018).

[17] M. Otteneder *et al.*, Nano Lett. **20**, 7152 (2020).

[18] X. Lu *et al.* arXiv:2006.13963.

[19] G. Tarnopolsky, A. J. Kruchkov, and A. Vishwanath, Phys. Rev. Lett. **122**, 106405 (2019).

[20] S. Becker, M. Embree, J. Wittsten, and M. Zworski, arXiv:2008.08489.

[21] S. G. Xu *et al.*, Nat. Commun. **10**, 4008 (2019).

[22] See Supplemental Material at http://link.aps.org/supplemental/10.1103/PhysRevB.103.165113 for contains mathematical details supporting the arguments presents in our manuscript.

[23] N. F. Mott and R. Peierls, Proc. Phys. Soc. **49**, 72 (1937).

[24] B. Roy and V. Juričić, Phys. Rev. B **99**, 121407(R) (2019).

[25] N. Dencker, J. Sjöstrand, and M. Zworski, Commun. Pure Appl. Math. **57**, 384 (2004).

[26] *Spectra and Pseudospectra: The Behavior of Nonnormal Matrices and Operators*, edited by L. N. Trefethen and M. Embree (Princeton University Press, Princeton, NJ, 2005).

[27] Y. Ren, Q. Gao, A. H. MacDonald, and Q. Niu, Phys. Rev. Lett. **126**, 016404 (2021).

[28] N. R. Walet and F. Guinea, 2D Mater. **7**, 015023 (2019).

[29] M. Zworski, *Semiclassical Analysis* (AMS, Providence, Rhode Island, 2012).

[30] K. Hejazi, C. Liu, H. Shapourian, X. Chen, and L. Balents, Phys. Rev. B **99**, 035111 (2019).

[31] L. Balents, SciPost Phys. **7**, 048 (2019).

[32] L. E. Thomas, Commun. Math. Phys. **33**, 335 (1973).

[33] All our results remain valid with the potentials U and V replaced by more general potentials, introduced in Ref. [22, (24)], that obey the same symmetries.

[34] J. M. B. Lopes dos Santos, N. M. R. Peres, and A. H. Castro Neto, Phys. Rev. Lett. **99**, 256802 (2007).

[35] L. Hörmander, *The Analysis of Linear Partial Differential Operators IV* (Springer, Berlin, Heidelberg, 1985).